High Impedance Fault Analysis in Transmission Line using S-Transform Analysis Different Types of Fault in Transmission Line

Anshu Bhakat
M.Tech Student
Electrical Engineering
Narula Institute of Technology
Kolkata, India

Nabamita Banerjee Roy
Associate Professor
Electrical Engineering
Narula Institute of Technology
Kolkata, India

Pratyusha Biswas Deb
Assistant Professor
Electrical Engineering
Narula Institute of Technology
Kolkata, India

***Abstract*:- In this paper, the application of S-transform for fault location in distribution networks has been considered. The S-transform is discovered to be applicable in transient based fault location in distribution networks. This technique is an expansion of Wavelet transform method and is based on a moving and scalable localizing Gaussian window. Taking into account this fact that the signal energy of faults has high amplitude around certain frequencies, the fault location can be identified considering the relationship between these frequencies and so-called path characteristic frequencies related to the fault traveling waves. The transient voltage signal energy is calculated using S-Transform. In order to demonstrate the effectiveness of the proposed method, conventional distribution networks and combined system (with overhead lines and underground cables) as two case studies have been evaluated. The IEEE 34-bus test distribution network is simulated in EMTP-RV software and the relevant S-transform analysis is carried out in MATLAB coding environment.**

Keywords: Time frequency analysis kit; High Impedance Faults system; MATLAB Simulink, S-Transform, Time measurement kit

I. INTRODUCTION:

A novel method for high impedance fault (HIF) detection based on pattern recognition systems is presented in this paper. Using this method, HIFs can be discriminated from insulator leakage current (ILC) and transients such as capacitor switching, load switching (high/low voltage), ground fault, inrush current and no load line switching. Wavelet transform is used for the decomposition of signals and feature extraction, feature selection is done by principal component analysis and Bayes classifier is used for classification. HIF and ILC data was acquired from experimental tests and the data for transients was obtained by simulation using EMTP program.

Results show that the proposed procedure is efficient in identifying HIFs from other events. A new method for high impedance fault detection is proposed in this paper. Stockwell transform is used to extract the third harmonic current phase angle, measured only at the substation, whereas the moving standard deviation continuously monitor this parameter.

The fault is detected when the standard deviation is below a self-adaptive threshold for a predetermined period of time. To validate the method, a real distribution network is adopted, considering a modelled stochastic noise based on real current signals.

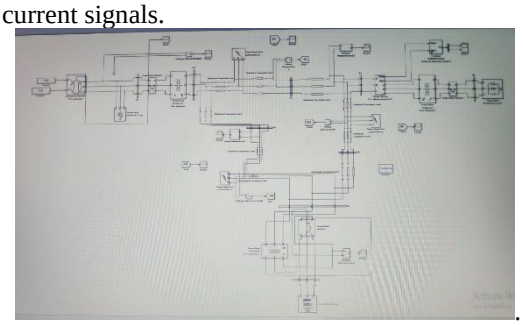

Fig. Analysis of HIF faults using MATLAB

II. THE S-TRANSFORM:

A. The Standard S-Transform:-

The S-transform is a time-frequency analysis technique proposed by Manisha et al. combines both properties of the short time Fourier transform and wavelet transform. It provides frequency dependent resolution while maintaining a direct relationship with the Fourier spectrum. The S-Transform of a signal x (t) is defined as:

$$S(\tau, f) = \int_{-\alpha}^{\alpha} x(t)\{\frac{|f|}{\sqrt{2\pi}} e^{-\frac{(r-t)^2 f^2}{2}} e^{-j2\pi f t}\}\, dt$$

Where the window function is a scalable Gaussian window

$$w(t, f, \delta) = \frac{|f|}{\sqrt{2\pi \cdot \delta}} e - \frac{t^2 f^2}{2\delta^2}$$

Combining equation (2) and (3) give:

$$s(rf\delta) = \int_{-\infty}^{\infty} x(t) \frac{|f|}{\sqrt{2\pi\delta}} e - j2\pi f t\ dt$$

The advantage of S-transform over the short time Fourier transform is that the standard deviation σ (f) (window width) is a function of f rather than a fixed one as in STFT. In contrast to wavelet analysis the S-Transform wavelet is divided into two parts as shown within the braces of equation (4).One is the slowly varying envelope (the Gaussian window) which localizes the time and the other is the oscillatory exponential kernel e−j2πFt. It is the time localizing Gaussian that is translated while keeping the oscillatory exponential kernel stationary which is different from the wavelet kernel. As the oscillatory

exponential kernel is not translating, it localizes the real and the imaginary components of the spectrum independently, localizing the phase as well as amplitude spectrum.

B. The Generalised S-Transform:-

The generalized S-transform is given by:

$$S(\gamma, f, \beta) = \int_{-\infty}^{\infty} x(t) w(\gamma - t, f, \beta) e^{-j_2 \pi f t}\, dt$$

Where w is the window function of the S-transform and β denotes the set of parameters that determine the shape and property of the window function. The window satisfies the normalized condition,

$$\int_{-\infty}^{\infty} w(t, f, \beta)\, dt = 1$$

The alternative expression of (5) by using the convolution theorem through the Fourier transform can be written as:

$$s(v, f, \beta) = \int_{-\infty}^{\infty} x(\alpha + f) w(\alpha, f, \beta) e^{j_2 \pi \alpha t}\, d\alpha$$

$$x(\alpha + f) = \int_{-\infty}^{\infty} x(t) e^{-j^2 \pi (\alpha + f)^t}\, dt$$

$$W(\pi, f, \beta) = \int_{-\infty}^{0} w(t, f, \beta) e^{-j^2 \pi \alpha t}\, dt$$

1. Proposed Scheme:

In this scheme we retain the window function as the same Gaussian window because it satisfies the minimum value of the uncertainty principle. We have introduced an additional parameter δ into the Gaussian window

Where its width varies with frequency as follows,

$$\sigma(f) = \frac{\delta}{|F|}$$

Hence the generalized S-transform becomes,

$$S(\gamma, f, \delta) = \int_{-\infty}^{0} x(t) \frac{|f|}{\sqrt{2\pi}\delta} e^{-\frac{(r-t)^2 f^2}{2\delta^2}} e^{-j^2 \pi f t}\, dt$$

Where the Gaussian window becomes,

$$W(t, f, \delta) = \frac{|f|}{\sqrt{2}\pi\delta} e^{-\frac{t^2 f^2}{2\delta^2}}$$

The adjustable parameter δ represents the number of periods of Fourier sinusoid that are contained within one standard deviation of the Gaussian window. The time resolution i.e. the event onset and offset time and frequency smearing is controlled by the factor δ. If δ is too small the Gaussian window retains very few cycles of the sinusoid. If δ is too high the window retains more sinusoids within it as a result the time resolution degrades at lower frequencies. It indicates that the δ value should be varied judiciously so that it would give better energy distribution in time-frequency plane. The trade-off between the time-frequency resolutions can be reduced by optimally varying the window width with the parameter δ. The variation of width of window with δ for a particular frequency component (25) Hz is shown in Figure.

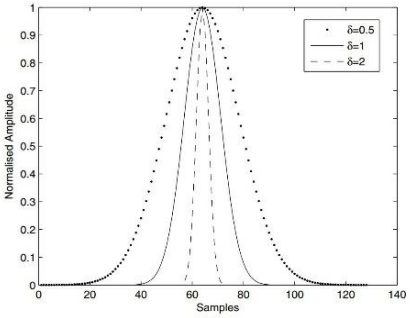

Fig. 1. Variation of window width with δ for a particular frequency (25Hz)

We varied the parameter δ linearly with frequency within a certain range as given by,

$$\delta(f) = ft$$

Where t is the slope of the linear curve. The discrete version of (11) is used to compute the discrete S-Transform by taking the advantage of the efficiency of the fast Fourier transform (FFT) and the convolution theorem.

2. The Discrete S-Transform:

Consider x (k T), k = 0, 1, ⋯, N be the discrete time series corresponding to x (t), with the sampling interval of T. So the discrete Fourier transform of x (k T) is given by

$$x\left[\frac{n}{NT}\right] = \frac{1}{N}\sum_{k=0}^{N-1} x(kT) e^{-\frac{j^2 \pi n k}{N}}$$

Where n = 0, 1, ⋯, N – 1 Using the discrete form of (11) the modified S-transform of the discrete signal x (kT) is given by (letting f ⟶ n/NT and τ ⟶ UT)

$$S\left[\frac{a}{NT} uT\right] = \sum_{m=0}^{N-1} X\left[\frac{m+n}{NT}\right] H(n, m) e - \frac{j^{2\pi mu}}{N}$$

Where u, m and n = 0, 1, ⋯, N − 1 and H (n, m) = e the Gaussian function. This is equal to the average of the time domain signal. To compute the discrete form of the proposed S-transform the following steps are to be adapted.

1) Perform the discrete Fourier transform of the time series x (kT) with N points and sampling interval to get using the FFT routine. This is computed once.

2) Calculate the localizing Gaussian H [n, m] for the required frequency n/NT.

3) Shift the spectrum X for the frequency,

4) Repeats steps 3, 4 and 5 until all the rows of corresponding to all discrete frequencies (n-NT) have been defined.

3. Performance Analysis:

In this section the performance of the proposed method is analysed using some synthetic test signals. In the first test a signal containing a low frequency (7 Hz), a medium frequency (25 Hz) and a high frequency (65 Hz) burst is taken. All these components are short lived and present in different time and also a zero signal component present at time t=0.23 sec. The spectrum of the signal obtained by STFT, the standard S-transform and the proposed scheme is shown in Figures (3)-(5).The STFT provides uniform frequency resolution but poor time resolution for all the frequency components. The standard S-transform results perfect time resolution at high frequency but fails in low frequency and good frequency resolution at low frequency but smears in higher frequency as seen from the vertical stretching of time frequency signatures. All these defects are somehow overcome by our proposed scheme of S-transform. It provides better energy concentration in both time and frequency direction.

This signal is chosen because it contains hyperbolic and chirp frequency components which are crossed to each other. The frequency of the hyperbolic component decreases while the frequency of the linear chirp increases in time. So it is difficult to provide good resolution for both the components. The performance is compared for the three methods is shown in fig- (7) to (9). It reveals that both the STF and standard S-Transform fails to provide

good resolution the high frequency of the hyperbolic and chirp component.

4. Application of s-transform in analysis of High Impedance Fault:

The generator bus outgoing currents are performed and approximate and detail coefficients and the process is carried out for both healthy and faulty conditions. Nine levels of decomposition of the current waveforms have been performed. After obtaining approximate and details coefficients in each level RMS, skewness and kurtosis values are computed. Hence, total six parameters are taken into account–skewness of approximate coefficient (SA), skewness of detail coefficient (SD), kurtosis of approximate coefficient (Ka), kurtosis of detail coefficient (KD), RMS of approximate coefficient (RMSa) and RMS of detail coefficient (RMSd). In the entire DWT analysis, Daubechies4 (DB4). S transform is considered as the mother wavelet. Each generator bus outgoing current is analysed separately. Percentage deviation of all the above mentioned parameters are calculated from their corresponding healthy condition values are calculated.

$$\%\ Deviation = \left|\frac{(Healthy\ value)\ -\ (Faulty\ value)}{Healthy\ value}\right| \times 100$$

A. Observation from generator Bus 1:

Percentage deviations of SA, SD, KA, KD, RMSa and RMSd are calculated and shown in Table A.1–A.6 (Appendix). Data given in the earlier mentioned tables have been presented in the form of graphs in Figures 2-4. From Figure 2(a) it has been noticed that when LG fault occurs at Bus 5, percentage deviation of SA at 6th level of decomposition is the greatest amongst all the parameters in all the levels. Figure 2(b) shows that for LL fault at Bus 5, greatest amount of percentage deviation occurs in RMSd at level 3.

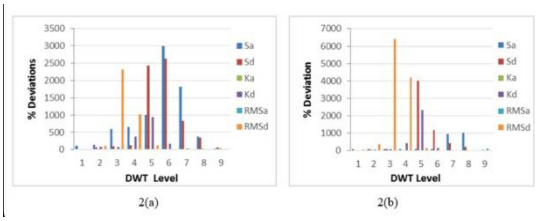

Fig-1. Percentage deviation of different parameters of GEN Bus 1 for (a) LG fault at Bus 5 and (b) LL fault at Bus 5

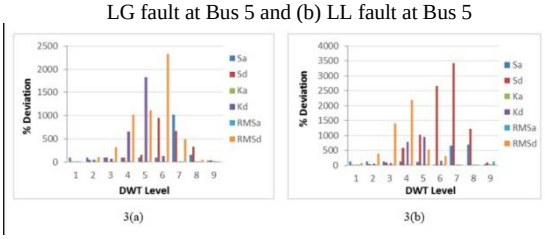

Fig-2. Percentage Deviation of different parameters of GEN Bus 1 for (a) LG fault at Bus 6 and (b) LL fault at Bus 6

From Figure 2 shows that percentage deviation of RMSd at level 6 is the greatest when LG fault takes place at Bus 6. Figure 3(b) shows that for LL fault at Bus 6, percentage deviation of SD at 7th level of decompositions becomes the greatest amongst all the parameters in all the levels.

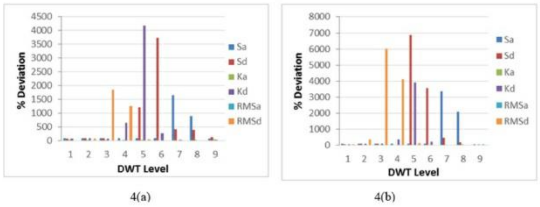

Fig-3. Percentage deviation of different parameters of GEN Bus 1 for (a) LG fault at Bus 8 and (b) LL fault at Bus

From Figure 3 shows that when LG fault occurs at Bus 8, percentage deviation of KD at level 5 is the greatest amongst all the parameters. Figure 4(b) suggests that for LL fault at Bus 8, greatest amount of percentage deviation occurs in SD at level 5.

B. Observation from Bus-bar Diagram:

The simulation model is developed using EMTP program. The power system under study. The simulated transformer is a three phase power transformer with the rating of 31.5MVA, 132/33 kV. The primary winding has 980 turns wound in 10 layers and the secondary winding has 424 turns wound in 4 layers. The transmission line has been modelled by two identical sections. The algorithm has been implemented on MATLAB environment and the inputs are differential currents derived from EMTP software.

Various operating conditions are simulated and the differential currents are obtained from secondary of the current transformers. Typical differential currents and time-frequency contours are illustrated in Figs. (1-3). Differential current and it's time-frequency contours for an inrush current is presented in Fig.1. As it is clear, the contours are interrupted and there is a consistent time interval between two lobes. Fig.2 shows differential current and time-frequency contours for internal turn to turn fault. Unlike inrush current, the contours are regular and they are not interrupted. A typical differential current for transformer energizing while turn to turn fault, is shown in Fig.3. As it is seen, the time-frequency contours are the same as the internal fault case. In order to investigate noisy conditions, random noise with SNR up to 20dB has been added to the differential current signals. The results are shown in Figs. 4-6. These cases are the same as cases that shown in Figs. 1-3, but are contaminated with noise. It is found, the time-frequency contours are less influenced by noise.

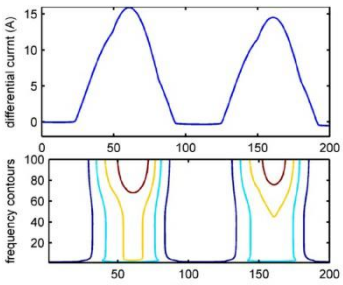

Fig-1. Differential current and S-contours for a magnetizing inrush current with no load

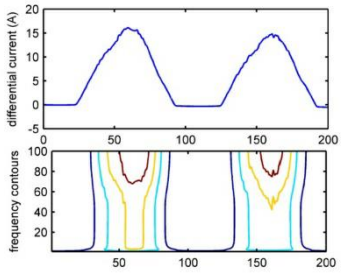

Fig-2. B-phase differential current and S-contours for internal fault between turns of primary winding

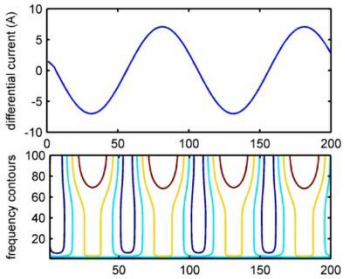

Fig-3. B-phase differential current and S-contours for inrush current while turn to turn fault between two turns

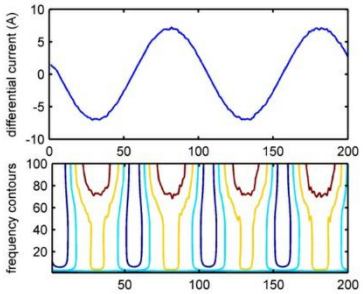

Fig-4. Differential current with SNR and S-contours for a magnetizing inrush current with no load

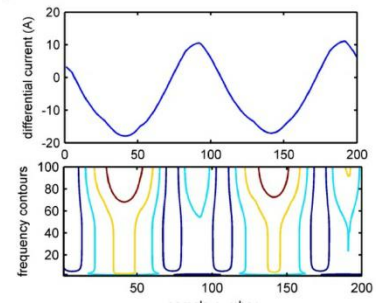

Fig-5. B-phase differential current with SNR and S-contours for internal fault between turns of primary winding

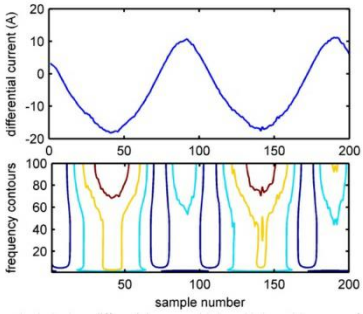

Fig-6. B-phase differential current with SNR and S-contours for inrush current while turn to turn fault between two turns

III. RESULTS AND DISCUSSION:

The FT study showed that there are inter harmonics in all HIF signals analysed. It is noticeable that harmonics and inter harmonics were present in all signals, with the prevalence of certain frequencies, showing that FT can be used to characterize HIFs properly. In addition, it is possible to observe that, since the HIF signal presents great variation over time, consequently there will be a change in the energy value in of each harmonic frequency.

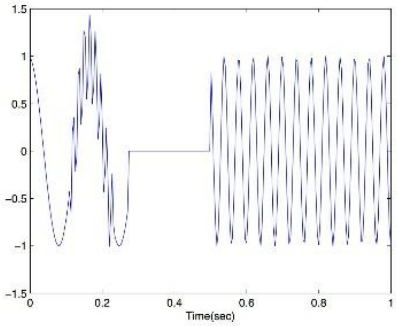

Fig. 2. First Test signal x1(t)

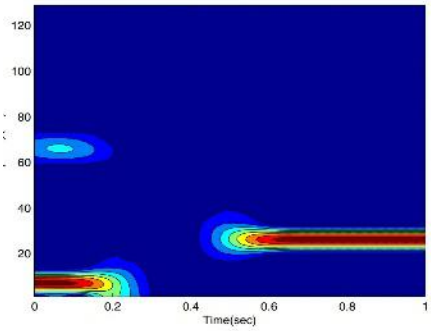

Fig. 3. STFT of x1(t)

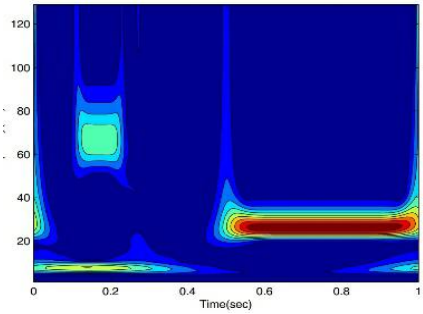

Fig. 4. Standard S-Transform of x1(t)

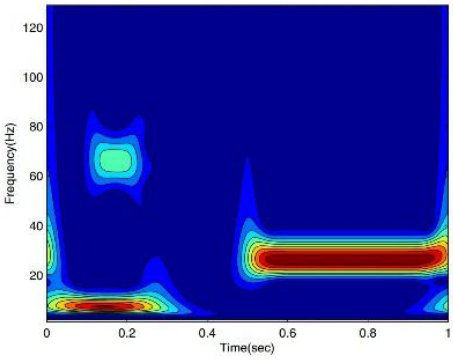

Fig. 5. Proposed S-Transform of x1(t)

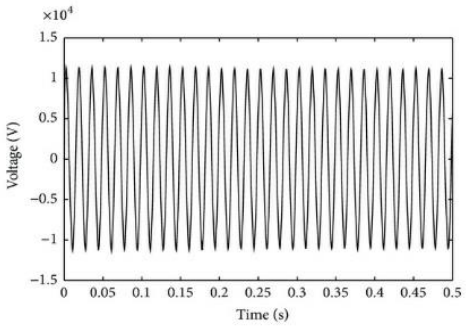

Fig. 6. Second Test signal x2(t)

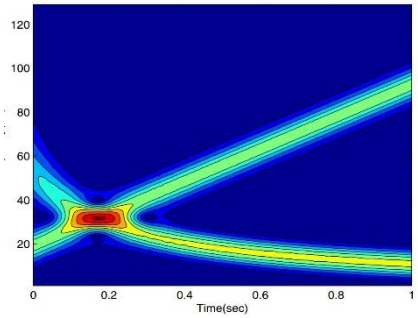

Fig. 7. STFT of x2(t)

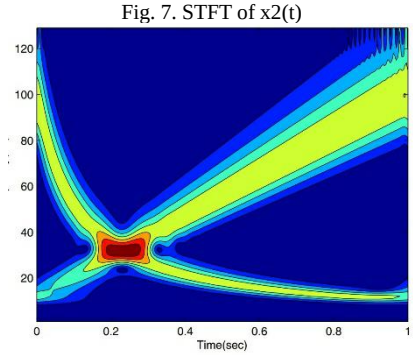

Fig. 8. Standard S-Transform of x2(t)

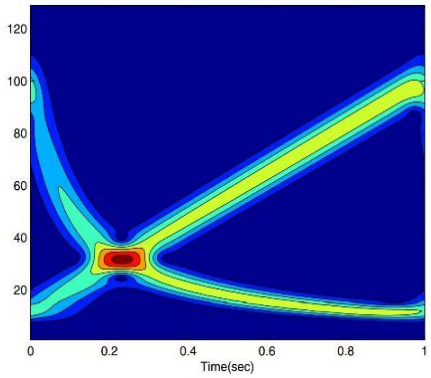

Fig. 9. Proposed S-Transform of x2(t)

IV. CONCLUSION:

In this paper we have proposed a modified S-Transform with improved time-frequency resolution. This has been achieved by introducing a modified Gaussian window which scales with the frequency in an efficient manner such that it provides improved energy concentration of the S-Transform. The effective variation of the width of the Gaussian window has a better control over the energy concentration of the S-Transform. This has been possible by introducing an additional parameter (δ) in the window which varies with frequency and thereby modulates the S-Transform kernel efficiently with the progress of frequency. The proposed scheme is evaluated and compared with the standard S-transform and STFT by using a set of synthetic test signals. The comparison shows that the proposed method is superior to the standard one as well as STFT.

A. AUTHORS AND AFFILIATIONS:

The paper was collaborative effort among the authors. The authors contributed collectively to the theoretical analysis and manuscript preparations**.** That is collected with the help of Dr. Rajesh Mallik, Department of Electrical and Electronics Engineering, Indian Institute of Technology, Roorkee, Haridwar, Uttarakhand, 247667, India**.**

B. CONFLICTS OF INTEREST:

The author declare no conflict of interest.

V. ACKNOWLEDGMENT:

The authors were extremely benefited from frequent discussions with Pratyusha Biswas Deb, Asst. Prof of Narula Institute of Technology, Kolkata.

REFERENCES:

[1] Stockwell RG, Manisha L, and Lower RP Localisation of the complex spectrum: the S transform, IEEE Trans Signal Processing 1996; 44(4), p p: 998-1001

[2] Stockwell, R. G. , S-Transform Analysis of Gravity Wave Activity, Ph.D. Dissertation, Dept. of Physics and Astronomy, The University of Western Ontario, London, Ontario, Canada,1999.

[3] Michael R. Port off, Time-Frequency Representation of Digital Signals and Systems Based on – Short Time Fourier Analysis, IEEE Transactions On Acoustics, Speech, And Signal Processing, Vol. Asp–28, No. 1,February 1980.

[4] Ingrid Daubechies, The Wavelet Transform, Time-Frequency Localization and Signal Analysis, IEEE Trans. On Information Theory, Vol.36, No.5, and pp: 961–1005, Sep 1990.

[5] P.K. Dash, S.R. Samantaray, G. Panda and B.K. Panigrahi, Power transformer protection using S-transform with complex window and pattern recognition approach, IET Genre. Transom. Diatribe. Vol. 1, pp: 278–286, 2007.

[6] P. K. Dash, B. K. Panigrahi, D. K. Shoo, and G. Panda, Power Quality Disturbance Data Compression, Detection, and Classification Using Integrated Spline Wavelet and S-Transform, IEEE Transactions On Power Delivery, Vol. 18, pp: 595–600, April 2003.

[7] P Rakovi, E Sejdi, LJ Stankovi, J Jiang, Time-Frequency Signal Processing Approaches with Applications to Heart Sound Analysis, Computers in Cardiology ,Vol:33,pp:197200,2006.

[8] C.R. Pinner, Time frequency and time filtering with the S-transform and TT-transform, Digital Signal Processing 15 (2005) 604-620.

[9] Lush B. Almeida, The fractional Fourier transform and time-frequency representations, IEEE Trans. Signal Processing 42 (11), pp: 3084-3091, 1994.

[10] K. F. Tempo, Dewitt Assai, J. Fended, L. Manisha, and H. Rasmussen, Post seismic Deformation Following the 1994 Northridge Earthquake Identified Using the Localized Hartley Transform Filter, Pure Applied Geophysics. 165 (2008) 1577-1602.

[11] P. D. Mc Fadden, J. G. Cook, and L. M. Forster, Decomposition of gear Vibration signals by the generalized S-transform, Mechanical Systems and Signal Processing, vol. 13, no. 5, pp.691-707, 1999.

[12] P. K. Dash, B. K. Panigrahi, and G. Panda, Power quality analysis using S-transform, IEEE Transactions on Power Delivery, vol. 18, no. 2, pp.406411, 2003.

[13] C. R. Pinner and L. Manisha, Time-local Fourier analysis with a scalable, phase-modulated analysing function: the S Transform with a Complex window, Signal Processing, vol. 84, no. 7, pp. 11671176, 2004.
[14] C. R. Pinner and L. Manisha, The bi-Gaussian S transform, SIAM Journal of Scientific Computing, vol. 24, no. 5, pp. 16781692, 2003.
[15] C. R. Pinnegar and L. Manisha, the S-transform with windows of Arbitrary and varying shape, Geophysics, vol. 68